

Probing the nodal gap in the pressure-induced heavy fermion superconductor CeRhIn₅

Tuson Park^{1,2}, E. D. Bauer¹, and J. D. Thompson¹

¹ *Los Alamos National Laboratory, Los Alamos, New Mexico 87545, USA*

² *Department of Physics, Sungkyunkwan University, Suwon 440-746, Korea*

(Dated: February 2, 2022)

We report field-orientation specific heat studies of the pressure-induced heavy fermion superconductor CeRhIn₅. These experiments provide the momentum-dependent superconducting gap function for the first time in any pressure-induced superconductor. In the coexisting phase of superconductivity and antiferromagnetism, field rotation within the Ce-In plane reveals four-fold modulation in the density of states, which favors a d-wave order parameter and constrains a theory of the interplay between superconductivity and magnetism.

PACS numbers: 74.20.Rp, 71.27.+a, 74.25.Bt, 75.20.Hr

The emergence of superconductivity near an antiferromagnetic quantum critical point (QCP) suggests that magnetic fluctuations associated with the QCP may provide a glue to form electron pairs [1]. In unconventional superconductors, the superconducting (SC) order parameter, which is tied closely to the SC pairing mechanism, breaks the underlying crystalline symmetry and contains nodes at which the SC gap becomes zero on the Fermi surface. The presence of nodal quasiparticles qualitatively changes the density of states (DOS) at the Fermi level and leads to a power-law temperature dependence of thermodynamic properties [2]. This power-law behavior contrasts with the exponential temperature dependence in fully gapped conventional superconductors and, therefore, provides an indicator of unconventional superconductivity. Unambiguous determination of an unconventional SC order parameter, however, comes from phase-sensitive and momentum-dependent studies that, complemented by the thermodynamic measurements, have established a d-wave order parameter in high- T_c cuprates [3] and p-wave symmetry in Sr₂RuO₄ [4].

In heavy fermion superconductors, where the relationship between superconductivity and quantum criticality is most conspicuous [1], details of the SC gap are rarely available because of disorder from chemical substitution or pressure environments that are needed to induce superconductivity. In this Letter, we report field-orientation specific heat (C_p) measurements on the pressure-induced superconductor CeRhIn₅. When a magnetic field is rotated in the Ce-In plane, four-fold modulation in C_p is observed deep in the SC state, with minima along [100] that indicate gap zeros at this direction in a d-wave order parameter. These results provide the momentum-dependent SC gap function for the first time, which is also the first in any pressure-induced superconductor, and open a new avenue to insights on the pairing mechanism in strongly correlated superconductors.

CeRhIn₅ is an antiferromagnet below $T_N = 3.8$ K and belongs to a family of heavy-fermion compounds CeMIn₅

(M=Co, Ir, Rh) that become superconducting for M=Co and Ir at 2.3 and 0.4 K, respectively [5, 6, 7]. Derived from the antiferromagnet CeIn₃, it crystallizes in the tetragonal HoCoGa₅ structure, where a Ce-In plane and a M-In block are alternately stacked along the c-axis. When subjected to pressure, CeRhIn₅ becomes superconducting near 0.5 GPa where T_N starts to decrease, suggesting a correlation between superconductivity and magnetism (see Fig. 1a) [5, 8]. As shown in Fig. 1a, there are two critical pressures at 1.75 and 2.3 GPa denoted P1 and P2. Below P1, superconductivity and magnetism coexists on a microscopic scale, while a purely SC phase only appears above P1 [9]. P2 is a field-tuned quantum critical point hidden by the SC dome [8]. At pressures above P1, the zero-field nuclear spin-relaxation rate $1/T_1$ and specific heat show a power-law temperature dependence below T_c , which is similar to what is found in the ambient-pressure heavy-fermion superconductor CeCoIn₅ with a d-wave SC order parameter [9, 10, 11]. In the coexisting phase below P1, the temperature dependence of $1/T_1$ crosses over from T^3 to T -linear with decreasing temperature in the SC state, suggesting a change from d-wave singlet pairing to an exotic SC order parameter [12]. Singular quantum fluctuations in the vicinity of an AFM QCP also have been proposed to favor unconventional order parameters ranging from a p-wave singlet to extended d-wave with additional nodal points [13, 14].

Whereas power laws in $1/T_1$ and C_p are consistent with a nodal gap in the coexistence phase, these measurements are insensitive to the location of nodes. To resolve this important question, we have developed a field-rotation specific heat technique under pressure. Single crystals used in this study were obtained from a batch where a residual resistivity ratio (RRR) was measured routinely to be of the order of 500, indicating exceptional sample quality. A hybrid clamp-type pressure cell made of Be-Cu/NiCrAl and silicone-fluid transmitting medium were used to produce hydrostatic pressure environments up to 2.5 GPa. The superconducting transition temperature of Sn was measured inductively to determine the pressure

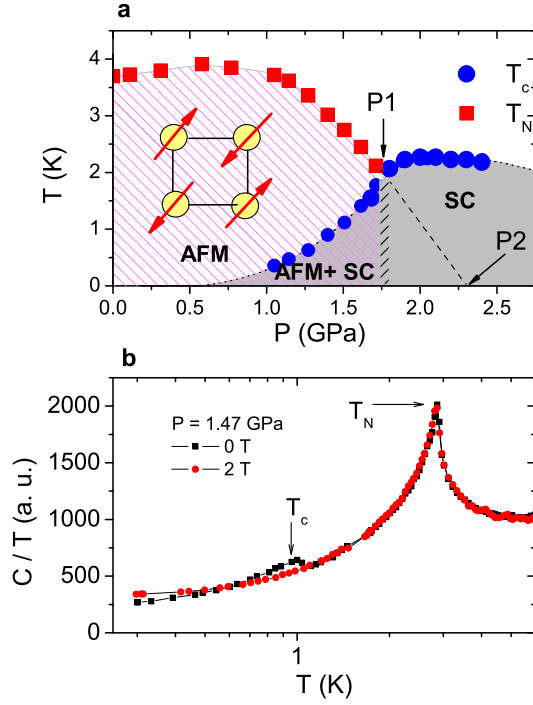


FIG. 1: (color online) **a** Phase diagram of CeRhIn₅ as a function of pressure [15]. Pressure induces a bulk superconducting (SC) state at 0.5 GPa that coexists with the antiferromagnetic (AFM) phase up to P1, where T_c becomes equal to T_N . The critical pressure marked by P2 is the field-tuned quantum critical point hidden by the SC dome. **b** Heat capacity of CeRhIn₅ at 1.47 GPa. The incommensurate AFM transition at 2.86 K is followed by a SC transition at 1.04 K. When 2 T is applied (circles), the magnetic transition is barely changed, while the superconductivity is completely destroyed.

at low temperatures. Magnetic field rotation was performed by using a triple-axis vector magnet with a large bore of 2.5" (American Magnetic Inc.) that accommodated a ³He cryostat with the pressure cell. Specific heat under pressure was measured by an ac calorimetric technique where ac heating incurs oscillation in the sample temperature (T_{ac}) that is inversely proportional to the sample's heat capacity, i.e., $T_{ac} \propto 1/C$ [16]. The oscillating temperature was measured by a Au-Fe/chromel thermocouple, which was attached to one face of the plate-like sample, while a constantan heater was glued to the opposite face. Magnetic field effects on the thermoelectric voltage of the Au-Fe thermocouple were determined independently.

Figure 1b shows the temperature dependence of the heat capacity of CeRhIn₅ in its coexisting phase at 1.47 GPa. Long-range magnetic order with wave vector $\mathbf{Q}=(0.5, 0.5, 0.297)$ appears at 2.86 K (T_N) and is robust against magnetic field; whereas, the SC transition occurs at 1.04 K (T_c) and is completely destroyed at 2 T ($H \parallel$ a-axis). The magnetic transition at this pressure is as sharp as it is at ambient pressure, indicating a negli-

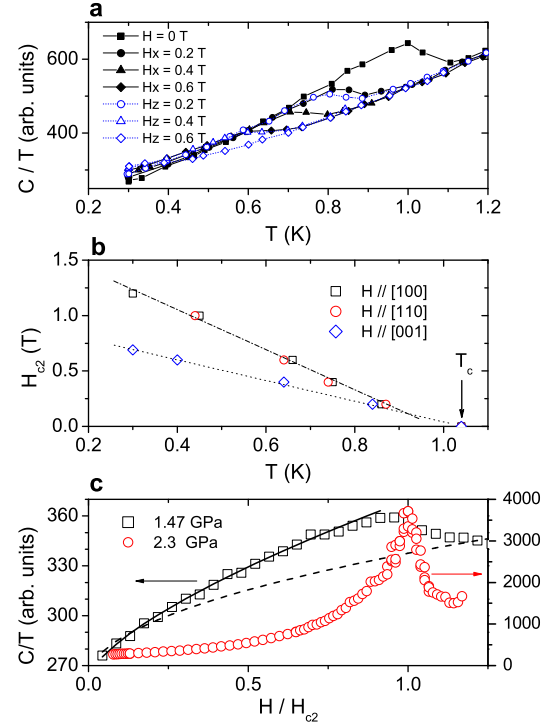


FIG. 2: (color online) **a** Low-temperature heat capacity (C_p) of CeRhIn₅ at 1.47 GPa and in low applied fields indicated in the legend. Solid and open symbols represent C_p/T for field along [100] and [001], respectively. **b** Temperature dependence of the upper critical field H_{c2} . Squares, circles, and diamond symbols correspond to fields along [100], [110], and [001], respectively. The dotted (or dash-dotted) line is a guide for a linear- H dependence. **c** Magnetic field dependence of C/T at 300 mK for $H \parallel [100]$ at 1.47 GPa (squares) and 2.3 GPa (circles). Here H_{c2} is 1.2 and 7.7 T for 1.4 and 2.3 GPa, respectively. The solid line describes least-squares fitting by $\Delta C/T = C/T - C(0T)/T = AH^n$ with $n = 0.68$, while the dashed line is for $n = 0.5$.

gibly small pressure gradient in the pressure cell.

The low- T heat capacity of CeRhIn₅ is shown in Fig. 2a for representative fields along [100] (solid symbols) and along [001] (open symbols). These data allow a determination of anisotropy of the upper critical field H_{c2} . Within the ab-plane, the upper critical field H_{c2}^{ab} is essentially isotropic (see Fig. 2b), but H_{c2}^c along the c-axis is smaller by a factor of two, which reflects the tetragonal crystalline structure as found in CeCoIn₅ [17]. For magnetic field along any crystalline axis, H_{c2} reveals a linear- T dependence down to the lowest experimental temperature (0.3 K), which is different from CeCoIn₅ where Pauli paramagnetic effects dominate conventional orbital fields ($H_{c2}^{orb} = -0.73T_c dH_{c2}/dT$) and H_{c2} is smaller than H_{c2}^{orb} by a factor of 5 [18]. Considering the exceptional sample quality of CeRhIn₅ ($\rho_0 = 30 \text{ n}\Omega \cdot \text{cm}$), the lack of Pauli limiting may arise from the presence of AFM that allows a SC order parameter other than a spin singlet [19]. We also note a positive curvature in H_{c2}^{ab} near T_c , which may

be ascribed to multi-band effects since there are three major bands that contribute to charge conductivity in CeRhIn₅ [20].

Field dependence of the specific heat of CeRhIn₅ does not conform to expectations for conventional type-II superconductors. Figure 2c shows representative field-swept data at 300 mK for H along [100] at 1.47 GPa (squares) and at 2.3 GPa (circles). In fully gapped conventional superconductors, C/T , which is proportional to the density of states (DOS), linearly depends on magnetic field because contribution to the DOS comes from quasiparticles generated inside vortex cores and the number of vortices is proportional to H . In unconventional superconductors with nodes, however, C/T increases as \sqrt{H} because Doppler-shifted quasiparticles leak through the nodes and contribute to the DOS [21]. A power-law form of $C/T = C(0T)/T + AH^n$ was used to fit the field-dependent specific heat of CeRhIn₅ at 1.47 GPa and the solid line in Fig. 2c best describes the data with $n = 0.68 \pm 0.04$ for field along [100]. This anomalous behavior may reflect the interplay between superconductivity and coexisting antiferromagnetism [15, 22]. The field dependence of C/T at 2.3 GPa is strikingly different from that in the coexisting phase, showing a first-order like sharp feature at H_{c2} . The upper critical field of CeCoIn₅ also is first order below $T_c/2$, suggesting that CeCoIn₅ is similar to the high-pressure phase of CeRhIn₅ [8, 23, 24].

Figure 3 shows the field-angle specific heat of CeRhIn₅ at 1.47 GPa for field rotations ϕ (θ) within (perpendicular to) the Ce-In plane. In the paramagnetic state at 3 K, C/T is featureless as a function of angle (not shown). In the AFM state but above T_c (squares in Fig. 3a), C/T shows a broad feature around [010] that may reflect the presence of AFM domains below T_N ($=2.86$ K). Upon decreasing temperature below T_c ($=1.04$ K), a new modulation in $C(\phi)/T$ appears in the mixed SC state (circles in Fig. 3a). The four-fold modulation is distinctly different from the spectrum observed in the magnetic state, indicating that the new structure is not related to magnetism, but arises from the SC gap symmetry. A polar sweep at the same pressure, temperature and field (Fig. 3b) shows only a two-fold modulation that reflects the factor of two anisotropy in H_{c2} between the ab-plane and c-axis.

Field-rotation specific heat, which is proportional to the angle-dependent DOS at low temperature, probes the momentum-dependent SC gap function and identifies gap-zero directions in unconventional superconductors [25, 26, 27, 28]. In the Abrikosov state, supercurrent circulates around a vortex core and extended quasiparticles experience a Doppler energy shift, $\delta E \approx \mathbf{v}_s \cdot \mathbf{k}_F$, where \mathbf{k}_F is the Fermi momentum of the quasiparticles and \mathbf{v}_s is the supercurrent velocity. Derived from the Doppler effects that depend on the relative magnetic field orientation against nodal points on the Fermi surface, the DOS precisely reflects the anisotropic gap

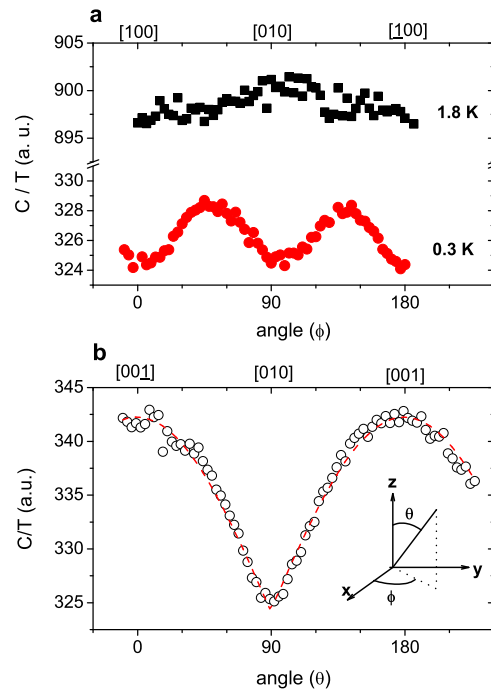


FIG. 3: (color online) Field-rotation specific heat of CeRhIn₅ at 1.47 GPa and 300 mK. **a** Azimuthal rotation (ϕ) of the magnetic field (0.5 T) within the Ce-In plane both in the AFM (1.8 K) and the coexisting phase of AFM and SC (0.3 K). **b** Polar rotation (θ) of the magnetic field (0.5 T) perpendicular to the Ce-In plane in the coexisting phase at 0.3 K. The solid line is a least-squares fit to a two-fold modulation model: $C = C_0 + A(1 + A_2 \cos \phi)$ with $C_0 = 265$, $A = 59.3$, and $A_2 = 0.30$, where the oscillation arises from H_{c2} anisotropy.

and modulates with field-rotation angle such that the DOS is minimal for field along nodal points but is maximal for field along antinodes [25]. Contributions to the field-rotation specific heat can be written as $C_{total}(\phi) = C_0 + C_2(\phi) + C_4(\phi)$, where the constant C_0 is the zero-field specific heat arising from thermally excited quasiparticles and phonons, the two-fold $C_2(\phi)$ comes from sample misalignment, and $C_4(\phi)$ describes modulation from the SC order parameter. The field-angle ϕ was determined against the crystalline a-axis or [100]. The lack of a two-fold oscillation indicates that the ab-plane is well matched with the field-rotation plane. Figure 4a is a plot of the field-induced heat capacity divided by temperature $\Delta C/T$ at 0.3 K and 1.47 GPa as a function of magnetic field angle, where $\Delta C = C_{total} - C_0 = C_4(\phi)$. Minima in ΔC can be approximated by a parabolic form $A(1 - A_4 \cos 4\phi)$ (dashed line) that is expected for a model gap structure of $\Delta(\theta, \phi) = \Delta_0 \sqrt{1 + \cos 4\phi}$ on a three-dimensional Fermi surface. Here θ is a polar angle determined against the c-axis or [001].

Figure 4b shows the four-fold oscillation amplitude A_4 at 0.3 K and 1.47 GPa as a function of magnetic field, which is obtained by a least squares fit to the sinusoidal form (dashed line in Fig. 4a). Compared to negligible H_{c2}

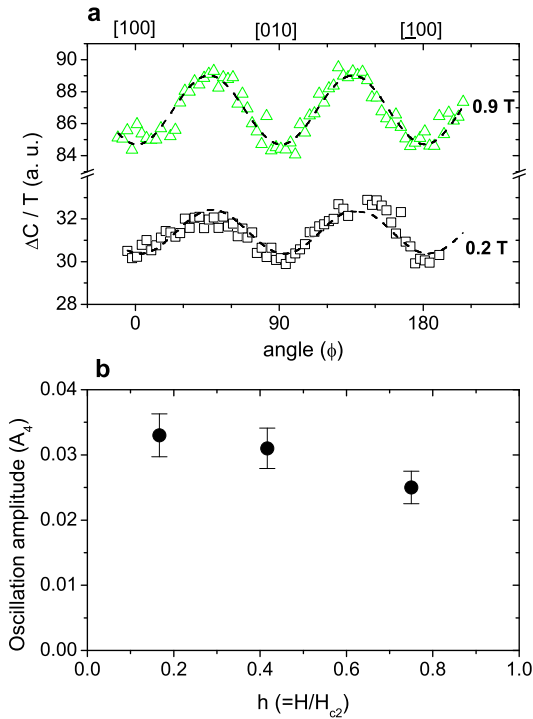


FIG. 4: (color online) **a** Field-rotation specific heat of CeRhIn₅ at 0.3 K for 0.2 (squares) and 0.9 T (triangles). Dashed lines are least-square fits by a sinusoidal form of the angular dependence (see text). **b** Oscillation amplitude A_4 as a function of the normalized field $h(= H/H_{c2})$ with $H_{c2} = 1.2$ T at 0.3 K.

anisotropy within the ab-plane (Fig. 2b), the large oscillation amplitude ($\approx 3.3\%$) in ΔC of CeRhIn₅ indicates that the four-fold modulation is not due to Fermi surface anisotropy, but due to symmetry of the SC gap function [27, 28]. Like CeCoIn₅, minima in ΔC of CeRhIn₅ are located along $\langle 100 \rangle$, indicating d_{xy} symmetry with line node along that direction [28]. In a recent theoretical treatment, however, Vorontsov and Vekhter argued that a reversal in the DOS anisotropy occurs at a critical field due to additional pair breaking from vortex scattering; consequently, minima along $\langle 100 \rangle$ in C_p can be interpreted instead as evidence for a $d_{x^2-y^2}$ gap [29]. A key future experiment to distinguish the two d-wave order parameters is to identify the critical field at which anisotropy reversal occurs in the field-rotation specific heat of CeRhIn₅.

These results constrain possible candidates of the SC gap in the coexisting phase of antiferromagnetism and superconductivity of CeRhIn₅. Four-fold modulation of the in-plane specific heat excludes an extended d-wave with additional nodes at points where the antiferromagnetic Brillouin zone crosses the Fermi surface, which was suggested to account for the T -linear $1/T_1$ at lowest temperatures [14]. A gapless p-wave spin-singlet state that was predicted [13] to be favored over a d-wave symme-

try near a QCP is also inconsistent with our observations. The two-fold modulation in specific heat under polar field sweeps, as shown in Fig. 3b, rules out the possibility of a hybrid gap with nodes at the poles, which has been suggested for CeIrIn₅ [31]. Instead, these results indicate a d-wave symmetry with line nodes along the c-axis.

To summarize, four-fold and two-fold modulations in representative in-plane and out-of-plane field-rotation specific heat measurements on CeRhIn₅ favor a d-wave SC order parameter over other suggested candidates in the vicinity of the quantum critical point, thus constraining a theory of the interplay between superconductivity and antiferromagnetism. This work will assure further studies of other pressure-induced superconductors where the nature of the SC order parameter has yet to be identified.

The authors thank I. Vekhter for discussion. Work at Los Alamos was performed under the auspices of the U.S. Department of Energy/Office of Science and supported by the Los Alamos LDRD program. T.P acknowledges a grant from the Korea Science and Engineering Foundation (KOSEF) funded by the Korea government R01-2008-000-10570-0.

-
- [1] N. D. Mathur *et al.*, Nature **394**, 39 (1998).
 - [2] G. E. Volovik, Pis'ma Zh. Eksp. Teor. Fiz. **58**, 457 (1993) [JETP Lett. **58**, 469 (1993)].
 - [3] D. J. Van Harlingen, Rev. Mod. Phys. **67**, 515 (1995).
 - [4] F. Kidwingira *et al.*, Science **314**, 1267 (2006).
 - [5] H. Hegger *et al.*, Phys. Rev. Lett. **84**, 4986 (2000).
 - [6] C. Petrovic *et al.*, J. Phys.: Condens. Matter **13**, L337 (2001).
 - [7] R. Movshovich *et al.*, Phys. Rev. Lett. **86**, 5152 (2001).
 - [8] T. Park *et al.*, Nature **440**, 65 (2006).
 - [9] T. Mito *et al.*, Phys. Rev. Lett. **90**, 077004 (2003).
 - [10] R. A. Fisher *et al.*, Phys. Rev. B **65**, 224509 (2002).
 - [11] W. K. Park, J. L. Sarrao, J. D. Thompson, and L. H. Greene, Phys. Rev. Lett. **100**, 177001 (2008).
 - [12] S. Kawasaki *et al.*, Phys. Rev. Lett. **91**, 137001 (2003).
 - [13] Y. Fuseya, H. Kohno, and K. Miyake, J. Phys. Soc. Jpn. **72**, 2914 (2003).
 - [14] Y. Bang, M. J. Graf, A. V. Balatsky, and J. D. Thompson, Phys. Rev. B **69**, 014505 (2004).
 - [15] T. Park *et al.*, Proc. Nat. Acad. Sci. (USA) **105**, 6825 (2008).
 - [16] P. F. Sullivan and G. Seidel, Phys. Rev. **173**, 173 (1968).
 - [17] R. Settai *et al.*, J. Phys: Condens. Matter **13**, L627 (2001).
 - [18] A. Bianchi, R. Movshovich, C. Capan, P. G. Pagliuso, and J. L. Sarrao, Phys. Rev. Lett. **91**, 187004 (2003).
 - [19] M. Sigrist and K. Ueda, Rev. Mod. Phys. **63**, 239 (1991).
 - [20] H. Shishido *et al.*, J. Phys. Soc. Jpn. **71**, 162 (2002).
 - [21] M. Ichioka, A. Hasegawa, and K. Machida, Phys. Rev. B **59**, 184 (1999).
 - [22] A. L. Cornelius, P. G. Pagliuso, M. F. Hundley, and J. L. Sarrao, Phys. Rev. B **64**, 144411 (2001).
 - [23] S. Ikeda *et al.*, J. Phys. Soc. Jpn. **70**, 2248 (2001).

- [24] H. Aoki *et al.*, J. Phys.: Condens. Matter **16**, L13 (2004).
- [25] I. Vekhter, P. J. Hirschfeld, J. P. Carbotte, and E. J. Nicol, Phys. Rev. B **59**, R9023 (1999).
- [26] T. Park, M. B. Salamon, E. M. Choi, H. J. Kim, and S. I. Lee, Phys. Rev. Lett. **90**, 177001 (2003).
- [27] P. Miranovic *et al.*, J. Phys.: Condens. Matter **17**, 7971 (2005).
- [28] T. Sakakibara *et al.*, J. Phys. Soc. Jpn. **76**, 051004 (2007).
- [29] A. Vorontsov and I. Vekhter, Phys. Rev. Lett. **96**, 237001 (2006).
- [30] A. Vorontsov and I. Vekhter, Phys. Rev. B **75**, 224501 (2007).
- [31] H. Shakeripour, M. A. Tanatar, S. Y. Li, C. Petrovic, and L. Taillefer, Phys. Rev. Lett. **99**, 187004 (2007).